Journal of Petroleum Science and Engineering 196 (2021) 108014

Contents lists available at ScienceDirect

Journal of Petroleum Science and Engineering

journal homepage: http://www.elsevier.com/locate/petrol

Observations on and use of curves of current dimensionless potential versus recovery factor calculated from models of hydrocarbon production systems

Milan Stanko

Department of Geoscience and Petroleum, Norwegian University of Science and Technology, S.p. Andersens Vei 15a. 7491, Trondheim, Norway

ARTICLE INFO

Keywords:
Current dimensionless production potential
Dimensionless production potential curves
Normalized maximum production versus recovery factor

ABSTRACT

In this work, curves of current dimensionless potential versus recovery factor are computed with models of hydrocarbon production systems. Additionally, a method to estimate production profiles using curves of current dimensionless potential versus recovery factor is presented. The author introduces three definitions, (1) the "production potential" is the maximum rate of hydrocarbon delivery for a production system at a given recovery factor. (2) The "maximum production potential" is defined as the maximum rate of hydrocarbon delivery at initial recovery factor. (3) The "current dimensionless potential" is defined as the production potential normalized by the maximum production potential. Several cases and modeling approaches, using coupled models of reservoir, well and gathering network are used. The reservoir was modeled using two approaches: a tank model (material balance equation) and a three-dimensional (3D) simulator. This work studies the effect of changes to the production system on the curve of current dimensionless potential, and how to handle such changes over the lifetime of the field when computing production profiles. It also discusses production scheduling using multiple curves of current dimensionless potential. Expressions and curves of current dimensionless potential versus recovery factor were derived using Arps decline equations and production data of a Norwegian offshore dry gas field.

Results show that the curve of current dimensionless potential is not affected significantly by (1) changes in number of wells, (2) initial surface volume in place, (3) layout of gathering system, (4) pipe and tubing diameter, (5) artificial lift and (6) formation permeability. However, the curve is strongly dependent on (1) reservoir drive mechanism, (2) model components considered in the flow-path from reservoir to separator and (3) model upstream and downstream boundary pressures. Curves of current dimensionless potential derived with the Arps exponential decline equation are similar to the results of the dry gas study case.

1. Introduction

Production profiles are one of the most important outputs calculated via models of hydrocarbon production systems. In the field design phase production profiles are calculated repeatedly and used extensively to size and design processing facilities, estimate the revenue profile, calculate net present value, among others (Haldorsen, 1996). In the production phase, input parameters to models are often adjusted to match measured data, to improve the fidelity of the model, and to reduce uncertainties. These tuned or history-matched models are then used to forecast future production and as input to design field modifications such as artificial lift implementations, infill drilling, enhanced oil recovery, improved oil recovery (Jahn et al., 2008).

Nowadays, models of hydrocarbon production systems are typically used by the oil and gas industry to compute production profiles. Those models often consist of a reservoir model and a steady-state well or gathering network model (Valbuena et al., 2015). The reservoir model computes the evolution in time of flow, saturation, and pressure in the porous media. The well and gathering network model compute equilibrium flow rates of oil, gas, water, and pressure and temperature in pipes and equipment. It has been discussed extensively in the past (e.g. Al-Shaalan et al., 2002) that neglecting or including the wellbore and gathering network model can have an important effect on the prediction of production profiles.

The reservoir and well and gathering network models are often run sequentially, where target rates and minimum pressure are imposed on the reservoir model. Then, the feasibility of the production rates is verified per time in the well and network model. Reservoir and well and gathering network models are often also coupled, where the well and gathering network model are converged in each time step of the

E-mail address: milan.stanko@ntnu.no.

https://doi.org/10.1016/j.petrol.2020.108014
Received 12 May 2020; Received in revised form 14 September 2020; Accepted 8 October 2020
Available online 14 October 2020

reservoir model (Barroux et al., 2000).

Models of hydrocarbon production systems are nowadays often built-in commercial software and have varying complexity. Some reservoir models the oil and gas industry typically employs are 3D reservoir simulators with thousand to million grid-blocks, material balance equation models or decline curve models. The 3D reservoir simulation is typically used for medium to large onshore and offshore fields with one operator. In contrast, the material balance equation models or decline curve models are typically used for medium to small reservoir units or for fields with fragmented owner- and operatorship.

Capacitance resistance models (CRM) are also often used to model production systems, e.g. to predict future performance of production systems, to perform reservoir characterization and evaluate inter-well connectivity using well production data and 4D seismic data. This family of models is based on building and solving systems of ordinary differential equations that represent reservoir depletion (often assuming a single or multi-tank model) and its interdependence with producers and injectors. A state-of-the-art review and an application example are presented by Holanda et al. (2018) and Yin et al. (2016), respectively.

3D reservoir simulators are often favored over other models (Ali and Nielsen 1970) to compute production profiles because they allow to include heterogeneities of the subsurface, well location and conditions. Additionally, they often have the option to model several relevant physical phenomena and it is often possible to tune them satisfactorily to measured data (partly due to the large number of model input parameters). Also, reservoir simulators are often integrated with other tools such as seismic interpretation and geological modeling software, making it possible to create reservoir volumes and seamlessly assign parameters and boundary conditions.

In most models of the production system, it is possible to compute a well's or field's maximum possible oil (or gas, depending on what is the preferred product) surface (standard conditions) rate at any given time. For example, in a system with chokes, this will be achieved by simulating each time-step with fully open chokes. This rate will be referred to hereafter as "production potential". The production potential is the upper bound of oil or gas rates possible to produce by the production system at current conditions. However, the production system can produce at this production potential (e.g. in declining fields) or at any value lower than that (e.g. fields producing at plateau).

The production potential will often be a function of cumulative production and injection only. For example, when using a material balance model for the reservoir, when there is a single reservoir flow unit and when using a pseudo-steady state inflow performance relationship (IPR) to represent the near well inflow. This is because, in a material balance model, reservoir pressure, and oil, gas and water saturations are often a function of cumulative production and injection only. Flowing gas oil ratios and water cuts are also a function of cumulative production and injection only. This is because they are often computed with the mobility ratio between the phases, which depend on the oil, gas, and water saturation of the tank. Therefore, wells' inflow performance relationships will also depend on cumulative production and injection only. Ultimately, the maximum production rates obtained with the well and gathering network model (that employ the wells' IPR as boundary conditions) will also depend on cumulative production and injection.

Injection strategies are usually dependent on production strategies and are often imposed using voidage replacement ratios or reinjection factors as a function of produced volumes. Therefore, it is often possible to express production potential as a function of cumulative production only.

The concept that a production system has a maximum feasible rate dependent only on cumulative production is also used when developing decline curve models, specifically when dealing with boundary dominated flow. Examples of analytical models and developments are presented in detail in Fetkovitch (1980). However, those approaches use mostly dimensionless time instead of cumulative production.

The observation that production potential depends on cumulative production only might not be valid for more complex cases. For example, when a 3D reservoir model is employed, the production potential is often not only a function of cumulative production but of how the reservoir has been produced until that point (e.g., when there is formation of gas or water coning). Moreover, there are often interactions between producers, injectors, structural features, drainage boundaries, and spatial effects.

Even for cases where a material balance is used to model the reservoir, the production potential might not be a function of cumulative production. For example, in low permeability formations that take considerable time to reach pseudo-steady-state or wells producing from different reservoir units but discharging to a common gathering network. Angga (2019) showed a case with two wells producing from different reservoir flow units where, for the same total cumulative production, the production potential depends on how much is produced from each unit.

Curves of production potential versus cumulative production can be used to generate production profiles (Gonzalez et al., 2019; Angga, 2019). An outline for calculation is as follows:

1. Define a time step, Δ_t
2. At time t_j, with the cumulative production and the production potential curve, read the maximum rate that the system can produce (the production potential)
3. If the desired target rate is higher than the production potential, then produce at production potential, if not, produce at target rate
4. Proceed to time t_{j+1}. Estimate the new cumulative production and repeat from step 2.

There might be variations of this method if cumulative production at t_{j+1} is estimated implicitly (using rate values of times t_j and t_{j+1}) or explicitly (using values of time t_j only).

The advantage of using production potential curves to estimate production profiles is that it is not necessary to run the model of the production system when varying target rates. Gonzalez et al. (2019) and Angga (2019) show that, by doing this, there is a minimal loss of accuracy. Therefore, it is often attractive to use production potential tables (or curves) as a proxy to production system performance in sensitivity, probabilistic and optimization studies. For example, Gonzalez et al. (2019) and Angga (2019) used production potential tables derived from coupled reservoir and production models in an optimization routine to determine optimal well and production schedule that maximize net present value.

However, if there are changes to the model input, such as initial volume in place, number of wells, formation permeability, etc., new potential production curves must be generated. Angga (2019) showed the effect changes in the initial volume in place have on the production potential curve. Generating new production potential curves requires running the original model repeatedly, which is time-consuming and often cumbersome. Thus, it is often worthwhile to simply use the original model rather than employing production potential curves.

It is also challenging to determine beforehand if using production potential curves is an appropriate method to reproduce future system performance. Moreover, production potential curves "lump" the performance of several wells; thus it is not possible to specify or determine how much each well produces.

There are two important research questions on this area that require further development: (1) how production potential curves affect by changes in the production system? (2) when (and how) can production potential curves be used to predict future performance of the production system?

The present work is addressing the first question, i.e. to study the behavior of the production potential versus cumulative production for several models' types and cases. To determine the affecting factors on the production potential curves, and determine the necessity for

recalculation. The present work also provides some examples, applications, and observations to the second question.

2. Curves of current dimensionless potential versus recovery factor

The author found that an effective way to conduct this research is to:

- Make dimensionless the production potential curve by (1) dividing values of current cumulative production by the initial volume in place (at standard conditions) and (2) dividing the values of current production potential by the maximum production potential ($q_{pp,max}$) when the production system transitions from zero to ultimate recovery factor. If there are no changes to the production system during the production horizon, $q_{pp,max}$ is usually registered at initial time "i", when recovery factor is zero. The resulting quantities will be referred to hereafter as "current dimensionless potential" and will be denoted using the symbol $\overline{q}_{pp}$.
- Run and extract the output directly from simulators, instead of deriving analytical expressions of the production potential (usually requires introducing simplifications).

To compute the curve of current dimensionless potential versus recovery factor using a model of a hydrocarbon production system, the author used the procedure below:

- Run a simulation and produce as much as possible during the whole life of the field. If the production system has adjustable components (e.g. wellhead chokes, electric submersible pumps, gas lift), the simulation should guarantee to produce as much as possible in every time step. Therefore, in some cases, e.g. with gas-lifted wells, optimization might be required in every time step to maximize hydrocarbon production rate by changing the settings of adjustable elements. At each simulation time, record the rate of the system (sum of all well's rates) and its corresponding cumulative production.
- Divide the recorded system produced rates by their maximum ($q_{pp,max}$, usually at time zero) and the cumulative production by the initial surface volume of hydrocarbons in place.

The shape and characteristics of the curve will depend on the type of system and model used. The next sections present and discuss some examples.

2.1. Study case 1: dry gas system, with a number of "x" identical wells producing from a common reservoir flow unit separately to their separator

An analytical model was developed using (1) the dry gas material balance, (2) the dry gas tubing equation, (3) the pseudo-steady state inflow backpressure equation with the "m" function,[1] and (4) the dry gas horizontal flowline equation. Heat transfer is neglected, and temperatures are assumed known throughout the system and independent of rate. The details of the model and the base case are provided in Appendix 1.

Calculations were performed for the base case (information provided in Appendix 1), and varying **independently** number of wells, initial gas in place (G), separator pressure (p_{sep}), tubing diameter (d_{tub}), product of formation permeability (k), layer height (h), initial reservoir pressure (p_{Ri}), reservoir temperature (T_R) and gas specific gravity (S_g). Results are shown in Fig. 1 a and b. The curves for different G's and number of wells are identical to the base case and are therefore not plotted.

The introduced input variations cause a modest variation in the field current dimensionless gas potential for the range of recovery factor between 0 and 0.6, with a maximum spread of +12% and −7% when compared against the base case. Separator pressure and initial reservoir pressure affect the curve significantly during the late life of the field. High initial reservoir pressures and low separator pressures cause an increase in the value of the recovery factor when current dimensionless potential equals zero. Low initial reservoir pressures and high separator pressures cause a decrease in the value of the recovery factor when current dimensionless potential equals zero.

Most cases had a different value of the upper bound of production potential ($q_{pp,max}$) and such value occurred at the recovery factor equal zero. For cases where the number of wells is varied, the upper bound of the production potential is proportional to the number of wells employed.

To evaluate further the effect of the well and gathering system on the shape of this curve, the author expanded the dry gas model with two additional scenarios:

- Neglect flow in tubing and separator pressure and consider the well backpressure inflow equation only, using a constant flowing bottom-hole pressure (p_{wf}).
- Wells are part of a gathering network where wells are arranged in templates, are identical and produce the same. This is achievable by using a common pipeline, identical flowlines from the template to a common entry point in the pipeline, and the same number of wells in each template.

The details of these two cases are provided in Appendix 1. The results are shown in Fig. 2. The presence of the gathering network did not significantly affect the curve when compared against the standalone case (the maximum deviation registered is +12% from the base case curve).

The presence of a system downstream the well bottom-hole does have a significant effect on the curve. If only an inflow performance relationship equation is considered and constant bottom-hole pressure is employed, the shape of the curve deviates from linear; thus, deviations from the base case become larger. Moreover, there is a significant impact on the values of recovery factor when current dimensionless potential equals zero.

If the bottom-hole pressure varies with depletion (i.e. with recovery factor), it is possible to match the curve of the base-case. The values obtained for the bottom-hole pressures that achieve matching are provided in Table 1.1 in the appendix.

The recovery factor where the current dimensionless field potential is zero ($R_{f,max}$) is the maximum theoretical recovery factor achievable from the field if it's produced until the rate drops to zero. In reality, fields will never reach this recovery factor because they are abandoned earlier when the minimum economic rate is reached.

$R_{f,max}$ strongly depends on the pressure assigned to the upstream and downstream boundaries of the model. For example, in Fig. 2, when the model considers IPR only, the $R_{f,max}$ varies from 0.66 to 0.89 when decreasing the flowing bottom-hole pressure. Surprisingly, the $R_{f,max}$ of the systems considering IPR only and standalone wells using the same downstream boundary pressure value of 30 bar is very similar.

In Fig. 1, for the production system with standalone wells the variation of separator pressure and reservoir pressure causes variations of $R_{f,max}$ between 0.79 and 0.96.

Changes in the surface layout of the gathering network, tubing diameter, well k h product, reservoir temperature and gas specific gravity have a negligible effect on $R_{f,max}$.

2.2. Study case 2: undersaturated oil reservoir with pot-aquifer undergoing gas or water injection

This study uses as a starting point for a model of the reservoir-well-gathering system built by Angga (2019) using commercial software

[1] The m function is the integral of pressure, p, divided by the product of viscosity, μ, times gas deviation factor, Z, from reference pressure to pressure of interest.

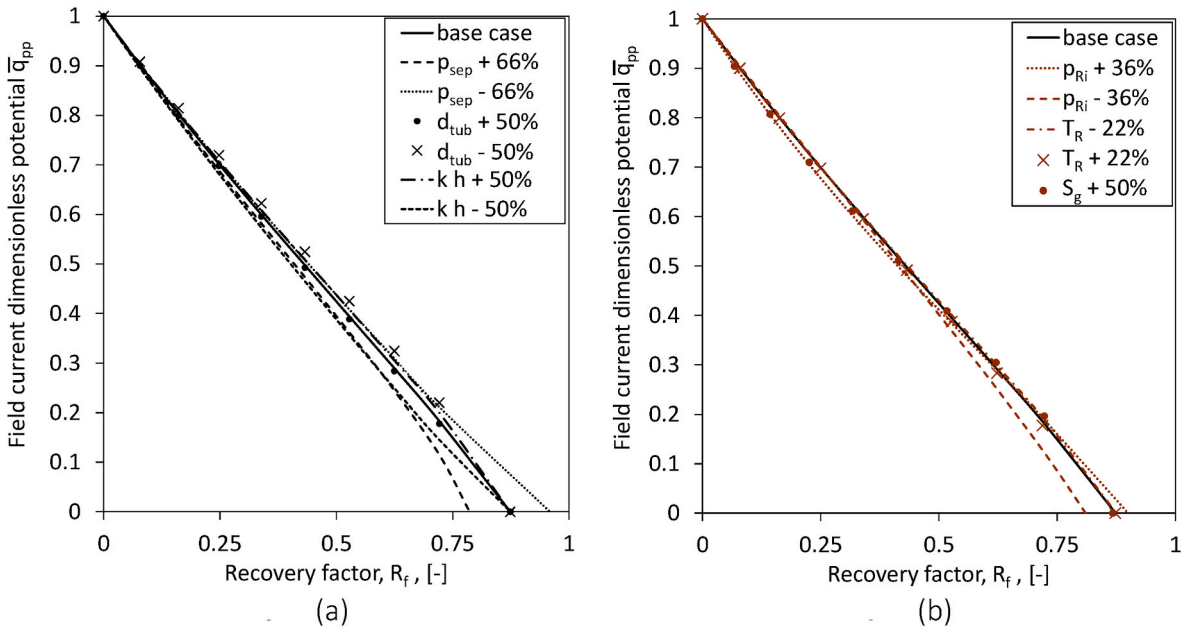

Fig. 1. Curve of field current dimensionless gas potential ($\bar{q}_{pp}$) vs, recovery factor (R_f), case: dry gas reservoir with standalone wells showing the effect of varying the following parameters: a) separator pressure (p_{sep}), tubing diameter (d_{tub}) and (k h) product b) initial reservoir pressure (p_{Ri}), reservoir temperature (T_R) and gas specific gravity (S_g). The effect of parameter variation on the curve is modest, except when varying separator and reservoir pressure.

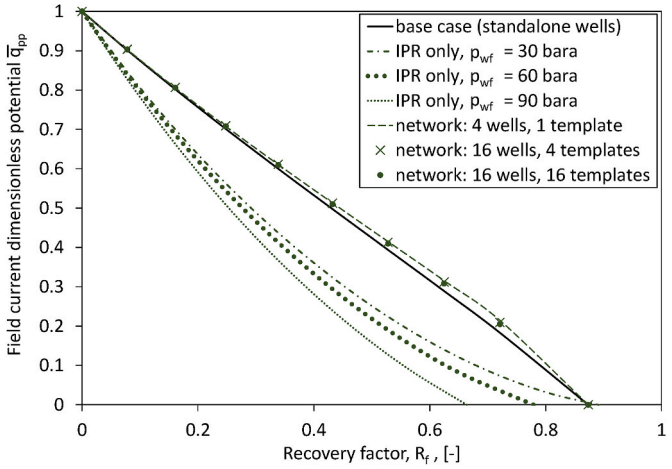

Fig. 2. Curve of field current dimensionless gas potential ($\bar{q}_{pp}$) vs recovery factor (R_f) for dry gas reservoir with standalone wells, network wells (with 4 wells-1 template, 16 wells-4 templates and 16 wells-16 templates) and considering inflow performance relationship (IPR) only and three values of flowing bottom-hole pressure (p_{wf}). The curves for standalone and network wells are similar, while the curves considering IPR only are different.

(Petroleum Experts, 2019). The reservoir was represented with a tank model, the well inflow performance with pseudo-steady-state equations, and the networks and well with steady-state pressure and temperature drop equations. Wells are equipped with gas lift valves, arranged in two clusters, one with 4 wells and one with 3. The production of the two clusters is commingled and sent to a pipeline, a riser that leads to the separator. The details of the model are provided in the work of Angga (2019) and repeated for clarity in Appendix 2.

The reservoir model has only one tank container that, at initial time, has both water (aquifer and connate water) and undersaturated oil. Injection of gas or water is estimated from produced volumes using input voidage replacement ratios (VRR).

The tank model and well and network models are coupled explicitly. Therefore, reservoir pressure, flowing water cut (W_c), and gas-oil ratio (R_p), oil, gas, and water mobilities (ratio between effective permeability and viscosity) are transferred at each time step from the tank model to the network model. IPR equations are updated with the mobility ratios. Flowing rates are calculated in the well and network models and are assumed constant until the next time step. In the next time step, the tank material balance is converged, and reservoir pressure, mobilities of oil, gas and water, and flowing R_p and W_c are computed. The process is then repeated.

The following cases were simulated:

2.1 Base case: Optimization of gas-lift rate allocation in every time step, flowlines from cluster 1 to pipeline entry and from cluster 2 to pipeline entry neglected. Water injection with voidage replacement ratio of 100%. 7 wells, all identical.

2.2 Base case but using different number of wells (varying between 1 and 6).

2.3 Base case but no gas lift.

2.4 Case 2.3 but doubling separator pressure.

2.5 Base case but with voidage replacement ratio of 75% instead of 100%.

2.6 Base case but increasing oil in place and pot aquifer size by 45%

2.7 Base case but decreasing oil in place and pot aquifer size by 45%

2.8 Base case but decreasing aquifer size by 45%

2.9 Base case but assigning different wells' productivity indexes (values provided in Appendix 2).

2.10 Same as case 2.9 but assigning lengths and diameters to flowline from cluster 1 to pipeline and cluster 2 to pipeline.

2.11 Base case but applying gas injection with 100% voidage replacement ratio, instead of water injection.

2.12 Same as case 2.3 but with gas injection and voidage replacement ratio of 100% instead of water injection.

2.13 Same as base case but with natural depletion.

The curves of the field current dimensionless potential versus recovery factor obtained from some of these cases that exhibit significant differences between them are shown in Fig. 3.

As observed in the dry gas case, input modifications related to the well, network system, reservoir and aquifer size cause none or modest variations of the base case curve. Therefore, cases 2.2,2.6,2.7,2.8,2.9 and 2.10 gave practically the same curve as case 2.1. Also, case 2.12

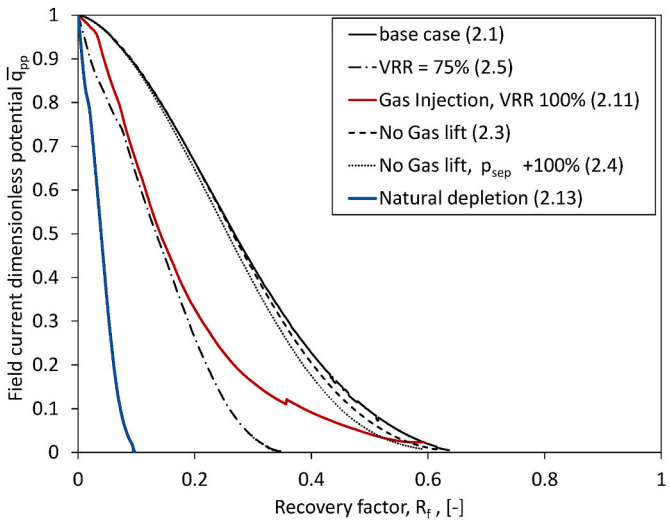

Fig. 3. Curve of field current dimensionless oil potential ($\bar{q}_{pp}$) vs. recovery factor (R_f), study case 2: Oil reservoir with network wells showing the following cases: water injection with voidage replacement ratio (VRR) of 100% (base case), water injection with VRR of 75%, gas injection with VRR of 100%, no gas lift, no gas lift with separator pressure (p_{sep}) doubled from the base case and natural depletion. The curve of the base case is greater than all others for all recovery factors.

gave similar results to 2.11. The biggest deviations were found when removing gas lift and doubling separator pressure.

Significant variations from the base case where detected if the recovery mechanism and strategy are modified. Cases with gas injection or using a voidage replacement ratio of 75% gave a curve very different from the base case.

The irregularities in the base case curve are due to convergence issues of the network solver in some time steps when using optimization to find optimal gas lift rates. The cause of the small step-jump that occurs in the curve corresponding to gas injection around recovery factor of 0.35 is unknown.

The recovery factor where the current dimensionless field potential is zero ($R_{f,max}$) was strongly dependent on the voidage replacement ratio employed.

2.3. Study case 3: undersaturated oil reservoir undergoing gas injection

This case uses as a starting point, a model of the reservoir-well-gathering system from the sample files of commercial software (Petroleum Experts, 2019). The model was modified to compute and output the production potential values and the injection network model was removed. The reservoir model has 21 × 20 X 10 cells (total 4200). The network and wells are modeled with steady-state pressure and temperature drop equations. Wells are equipped with wellhead chokes and are arranged in two clusters, with two wells each. The production of the two clusters is commingled and sent to a pipeline, a riser and finally reaches the separator. Some details of the model and the base case are provided in Appendix 3.

The reservoir model and well and network models are coupled explicitly. Therefore, well block pressure, flowing water cut, gas-oil ratio and inflow performance relationship tables are transferred from the reservoir model to the well and network model at each time step. Flow rates are calculated in the well and network models and are assumed constant until the next time step. In the next time step, the reservoir model is converged and reservoir pressure, saturation of oil, gas and water, flowing gas-oil ratio and water cut and IPR tables are computed. The process is then repeated.

The following cases have been simulated:

3.1 Base case: Gas injection with voidage replacement ratio of 84%.

3.2 Base case but using a porosity of 30% (porosity of base case is 25%), which gives an increase in N of 20%

3.3 Base case but reinjecting all produced gas.

The curves of current dimensionless potential versus recovery factor obtained from these cases are shown in Fig. 4. The curves of cases 3.1 and 3.2 overlap.

The gas injection case of study case 2 (case 2.11) was re-run but using a VRR equal to the base case of case 3.1 of study case 3. The plot of the two curves is given in Fig. 5. They are significantly different.

3. Applications of curves of field current dimensionless potential versus recovery factor

3.1. Computation of production profile

The curves of current dimensionless potential versus recovery factor can be used to estimate production profiles of the production system. This can be done by calculating first the production potential curves, i.e. the curves of production potential versus cumulative production. If the current dimensionless potential curve is available as a collection of points, a suitable procedure is:

- Multiply the values of current dimensionless potential by the maximum production potential, $q_{pp,max}$ (usually occurring at the initial time or recovery factor zero). The value of $q_{pp,max}$ can be found by solving the well and network model for initial reservoir pressure.
- Multiplying the values of recovery factor by the initial volume of hydrocarbons in place (Q).

With the curves of production potential available, field production profiles can be estimated from specified input field target rates, e.g using the procedure described in the introduction.

Often there are changes to the production system, either scheduled, e.g. when new wells are drilled during the lifetime of the field, well tubing is replaced, or updates of uncertain parameters, e.g. initial volumes in place. If these changes do not affect the curve of dimensionless potential, then it is only necessary to update $q_{pp,max}$ and/or Q to recompute production potential curves. This avoids having to re-run the model of the production system to generate new production potential curves. To find the new value of the upper bound of the production potential ($q_{pp,max}$), the well and network model must be run at initial

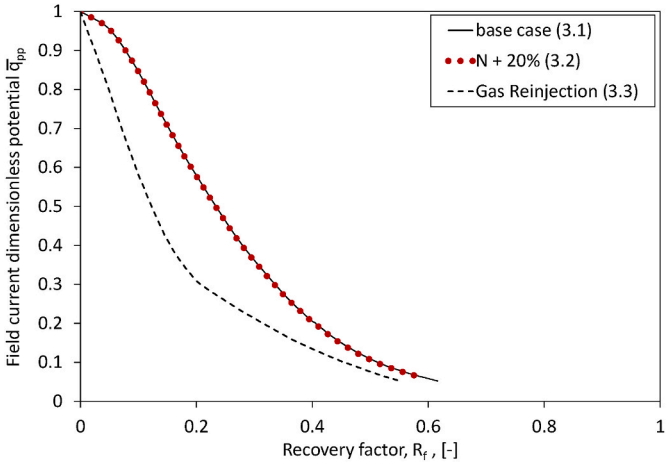

Fig. 4. Curve of field current dimensionless oil potential ($\bar{q}_{pp}$) vs. recovery factor (R_f), study case 3: Oil reservoir with network wells using a reservoir simulator showing the following cases: gas injection with voidage replacement ratio (VRR) of 84% (base case), gas injection with VRR of 84% and 20% higher initial oil in place, gas injection of produced gas. The curves for the base case and the case with higher initial oil in place are identical.

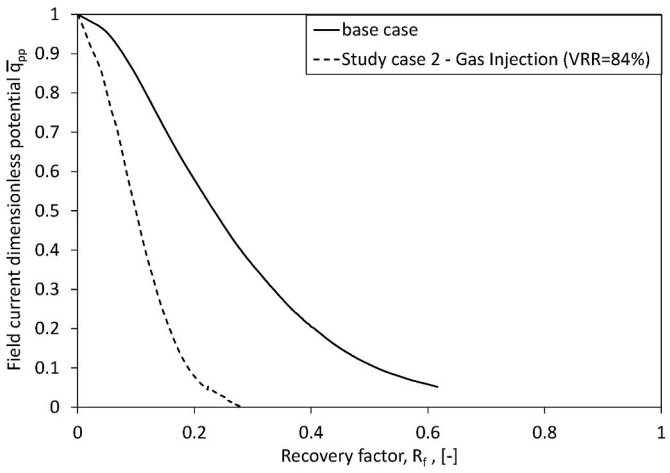

Fig. 5. Curve of field current dimensionless oil potential ($\bar{q}_{pp}$) vs. recovery factor (R_f), study case 3 – base case (gas injection with voidage replacement ratio of 84%) and study case 2 – gas injection with VRR = 84%. The figure shows that despite having the same voidage replacement ratio, the curves computed with the tank model and the reservoir simulator are different.

conditions with the changes to the production system included.

For example, using the results of the dry gas case (study case 1), the curve or current dimensionless potential versus recovery factor can be approximated to a straight line:

$$\bar{q}_{pp} = 1 - 1.163 \cdot R_f \quad (1)$$

Then, to calculate the production potential (q_{pp}) curve, one must multiply by $q_{pp,max}$, and substitute the definition of recovery factor:

$$q_{pp} = q_{pp,max} \cdot \left(1 - 1.163 \cdot \frac{G_p}{G}\right) \quad (2)$$

When there are changes to the production system during the lifetime of the field, e.g. well scheduling, updated production potential curves can be found by updating the value of $q_{pp,max}$ in Eq. (2).

If well scheduling (active producers) is changing with time, then it is necessary to compute $q_{pp,max}$ for all relevant combinations of wells producing and shut-in. For a system with "x" number of wells, where all combinations are relevant, this gives a total of 2^x cases. At each point in time, the proper $q_{pp,max}$ will be used to recompute production potential curves, depending on the active well schedule combination.

The selection of the proper value of $q_{pp,max}$ in time can be performed computationally by searching through a matrix (Table 1) that contains well status and $q_{pp,max}$ values:

3.1.1. Example: estimation of production profiles using the curves of current dimensionless potential versus recovery factor from case study # 3

The curve of current dimensionless potential versus recovery factor of the base case shown in Fig. 4 is used in this example. Three cases are computed and compared against the run of the coupled model:

1. Base case, plateau rate of 150 000 stb/d
2. Base case, plateau rate of 75 000 stb/d
3. Base case, with porosity of 0.3 and plateau rate of 75 000 stb/d

Results are shown in Fig. 6.

The prediction of production profiles using the current dimensionless potential versus recovery factor curve has an acceptable accuracy when compared against the rerun of the full coupled model. Maximum and average relative deviations (in percent) on the oil rate are 1.9% and 0.45% for case 1, 2.4% and 0.56% for case 2 and 1.91% and 0.49% for case 3.

A similar verification exercise comparing production profiles computed with production potential curves against reservoir simulation output is described in Gonzalez (2020) using the reservoir model of Gullfaks Statfjord oil.

Table 1
Table of relevant active and shut-in well combinations that are used in field well schedule and their maximum production potential. Example using 2 wells.

Case #	$q_{pp,max}$ [Sm^3/d]	Well 1 status	Well 2 status
1	$q_{pp,max,1}$	ON	ON
2	$q_{pp,max,2}$	OFF	ON
3	$q_{pp,max,3}$	ON	OFF
4	0	OFF	OFF

3.2. Estimating plateau duration and determining production split factor in a multi-reservoir field during early field planning

The author proposes the following procedure to estimate the plateau duration with the production potential curve. For a field producing with a constant plateau rate, the plateau period will end when the plateau rate becomes equal to the production potential of the field, $q_{pp}^* = q_{plateau}$. Therefore, using the production potential curve a cumulative production (Q_p^*) corresponding to $q_{plateau}$ can be found. Plateau duration (in days) is then computed by:

$$t_{plateau} = \frac{Q_p^*}{q_{plateau}} \quad (3)$$

As an example, Table 2 shows analytical expressions for current dimensionless potential versus recovery factor derived from the results obtained earlier for Case 1 (dry gas, base case) and Case 3 (oil with gas re-injection, case 3.3). Table 2 also shows production potential equations derived from the current dimensionless potential curves and plateau duration expressions.

In fields with several non-communicating reservoir flow units where the field is set to produce the desired plateau rate, sensitivity studies are often executed to determine optimal production split that provides maximum plateau duration. When all reservoirs are produced in plateau mode, the optimal production split will happen when all reservoirs enter

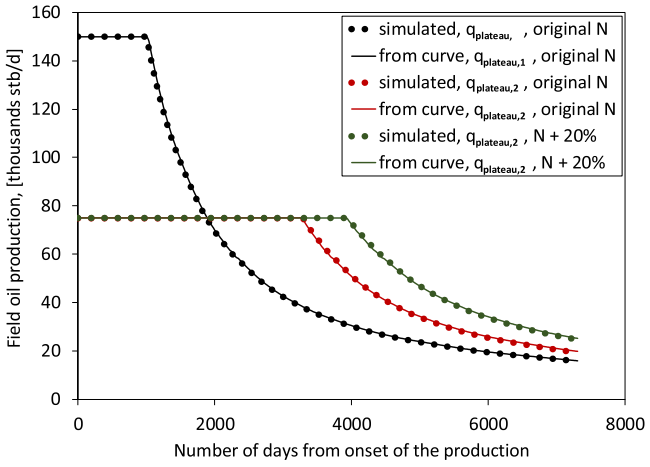

Fig. 6. Comparison of production profiles obtained using the curve of current dimensionless potential versus recovery factor and the full coupled model of reservoir simulator and wells and gathering network. The figure shows the following cases: original surface oil in place (N) with $q_{plateau,1}$ = 150 000 stb/d, original surface oil in place with $q_{plateau,2}$ = 75 000 stb/d and 20% higher original surface oil in place with $q_{plateau,2}$ = 75 000 stb/d. The production profiles computed with the simulator and the curves of current dimensionless potential are practically identical.

Table 2
Table of analytical expressions of current dimensionless potential vs recovery factors (fit to curves presented in Figs. 1 and 4), production potential and plateau duration.

	Case	
	Dry gas reservoir	Oil reservoir undergoing gas re-injection
Current dimensionless potential vs recovery factor	$\overline{q}_{pp} = 1 - 1.14 \cdot R_f$ (fitted to Fig. 1)	$\overline{q}_{pp} = e^{-5.17 \cdot R_f}$ (fitted to Fig. 4)
Production potential [Sm^3/d] versus cumulative production [Sm^3]	$q_{pp} = \left(1 - 1.14 \cdot \frac{G_p}{G}\right) \cdot q_{pp.max}$	$q_{pp} = e^{-5.17 \frac{N_p}{N}} \cdot q_{pp.max}$
Time at which plateau ends, in days	$t_{plateau} = \left(\frac{1}{q_{plateau}} - \frac{1}{q_{pp.max}}\right) \frac{G}{1.14}$	$t_{plateau} = ln\left(\frac{q_{pp.max}}{q_{plateau}}\right) \cdot \frac{N}{5.17 \cdot q_{plateau}}$

in decline at the same time. Optimal plateau rate splitting can be computed with the procedure described above by:

- Equating plateau duration for all reservoirs
- Add the additional constraint that the sum of all plateau rates must be equal to the desired field plateau
- Solve for reservoir plateau rates

For example, consider two reservoirs that follow the oil reservoir equations presented in Table 2, and with properties given in Table 3.

Equating the plateau duration of both reservoirs gives

$$ln\left(\frac{q_{pp.max,1}}{q_{plateau,1}}\right) \cdot \frac{N_1}{5.17 \cdot q_{plateau,1}} = ln\left(\frac{q_{pp.max,2}}{q_{plateau,2}}\right) \cdot \frac{N_2}{5.17 \cdot q_{plateau,2}} \quad (4)$$

And, using the condition that the sum of reservoir plateau rates should be equal to the field's plateau rate:

$$q_{plateau,1} + q_{plateau,2} = q_{plateau,field} \quad (5)$$

If desired $q_{plateau,field} = 25\,000$ Sm^3/d, then reservoir plateau rates to give same plateau duration are 10 349 and 14 651 Sm^3/d for reservoir 1 and 2 respectively, and plateau duration is 506 days.

4. Derivation of current dimensionless potential expressions from Arps decline equations

Conventional decline curve analysis often employs the empirical rate-time equations given by Arps (1945):

$$q(t) = \frac{q_i}{(1 + D_i \cdot b \cdot t)^{\frac{1}{b}}} \quad (6)$$

where b is a number between 0 and 1 indicating the type of decline, D_i is the initial decline rate and q_i is initial standard conditions rate. As suggested by Fetkovich (1980), in this derivation D_i will be approximated by:

$$D_i = \frac{q_i}{\left(\frac{1}{F}\right) \cdot Q} \quad (7)$$

The product $\left(\frac{1}{F}\right) \cdot Q$ represents the theoretical maximum amount of hydrocarbons that can be recovered from the reservoir. In the work of Fetkovich (1980) this product is equal to cumulative oil production to a reservoir shut-in pressure of 0 bara. In this work, the product is assumed to be equal to the cumulative production when the production system physically stops producing. Therefore, F is the inverse of the maximum "theoretical" recovery factor (recovery factor achieved when the system physically stops producing). The quantity F must always be greater or equal than 1 because it is not possible to produce more surface volumes of oil or gas than what is originally in place.

To obtain an expression of current dimensionless potential versus recovery factor, Eq. (6) is integrated from time 0 to current time t, to find cumulative production Q_p and then divided by initial hydrocarbon fluids in place Q. $q_{pp,max}$ is taken to be equal to q_i. The resulting equation is then rearranged to be a function of F, R_f and $\overline{q}_{pp}$ only. The results of this process are given in Table 4.

The equations obtained for the exponential and harmonic decline are identical in structure to the equations presented in Table 2 for the dry gas case and the undersaturated oil reservoir undergoing gas recycling.

Fig. 7 presents the plot of the equations presented in Table 4. The values of F used are the inverse of the recovery factor for when the current production potential is equal to zero ($R_{f,max}$) found for some of the study cases 1,2, and 3 presented earlier. The curves obtained are compared against the curves obtained previously for some results of study cases 1,2 and 3.

The expressions of current dimensionless potential versus recovery factor derived from Arps decline curve rate-time equations do not reproduce properly, for any value of b, the behavior of study cases 2 and 3. However, the exponential (b = 0) type curve successfully reproduces the results of study case 1. The behavior of the curve of study case 3 - gas reinjection - can be matched if the Harmonic decline equation (b = 1) is used, and the value of F is varied.

5. Computation of current dimensionless potential curves versus recovery factor from field data

The public production data of the Ormen Lange dry gas field, located offshore Norway, was used to generate the curve of current dimensionless potential versus recovery factor.

According to the website of the Norwegian Petroleum Directorate (Norwegian Petroleum Directorate, 2020), Ormen Lange has, since 2011, a total of 24 producers. The data of field production and cumulative production of the decline period (after 2012, at $G_p = 75$ E09 Sm^3 and above) was used to determine the maximum field potential at cumulative production zero (given in Table 5) by fitting a straight line through the peaks of the curve. Fig. 8 shows the plot of the current dimensionless potential versus recovery factor obtained with the field and the data of the base case of study case 1. The initial gas in place was varied to provide a reasonable match between the two curves. The value obtained (given in Table 5) is in the range discussed by Undeland (2012).

Table 3
Reservoirs' initial production potentials and initial oil in place.

	Reservoir 1	Reservoir 2
$q_{pp.max}$ [1E03 Sm^3/d]	30.00	40.00
N [1E07 Sm^3]	2.54	3.82

Table 4
Expressions of current dimensionless potential versus recovery factor derived from Arps decline curve rate-time equations.

Exponential (b = 0)	Hyperbolic (0 < b < 1)	Harmonic (b = 1)
$\overline{q}_{pp} = 1 - F \cdot R_f$	$\overline{q}_{pp} = (1 - F \cdot (1 - b) \cdot R_f)^{\frac{1}{1-b}}$	$\overline{q}_{pp} = e^{-R_f \cdot F}$

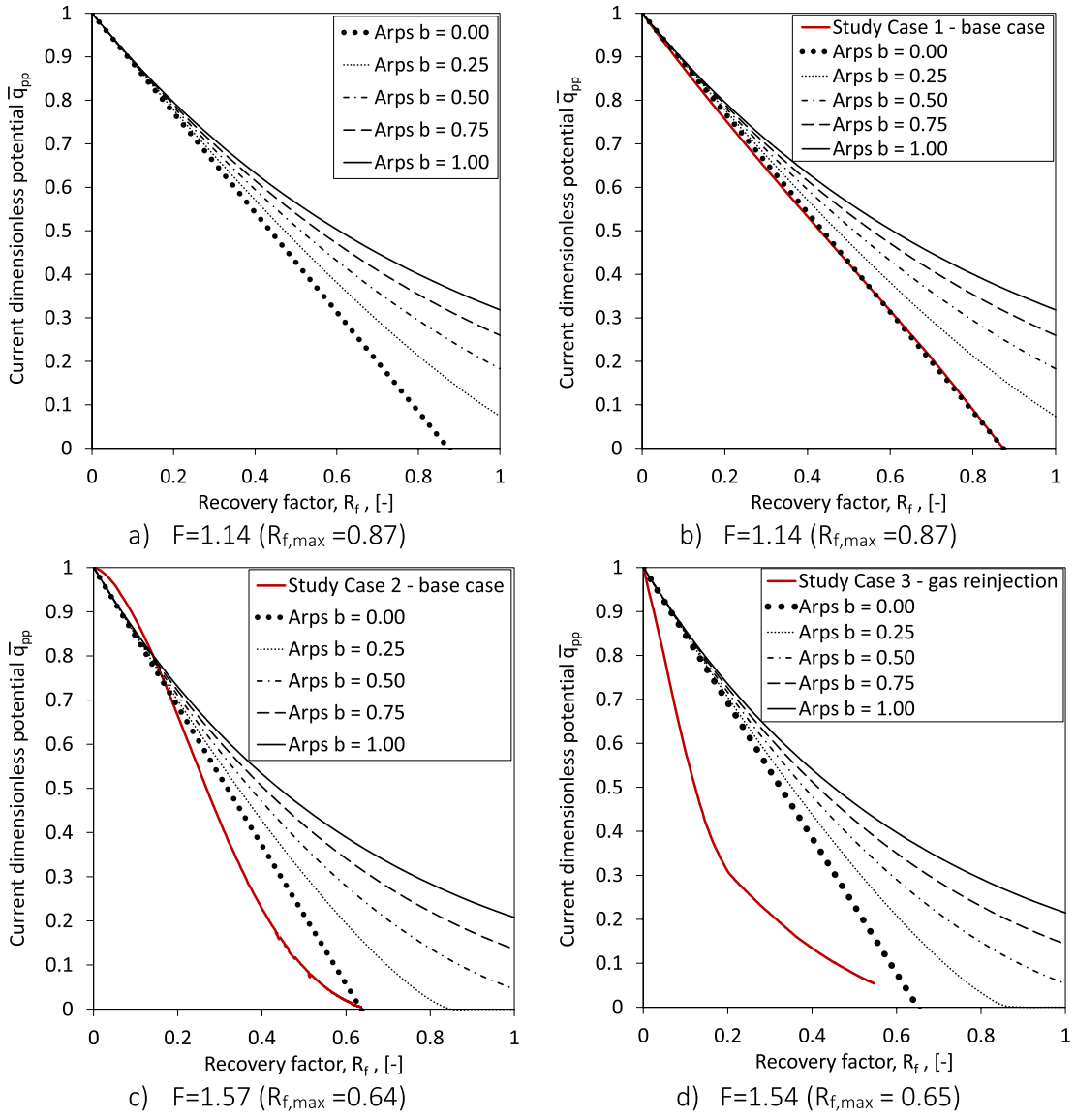

Fig. 7. Curves of current dimensionless potential ($\bar{q}_{pp}$) vs. recovery factor (R_f), derived from the decline curve rate-time equations of Arps, using b = 0, 0.25, 0.5, 0.75, 1, and F = 1.14 (Fig. 7a and 7 b), F = 1.57 (Fig. 7c) and F = 1.54 (Fig. 7d) compared against results of Study cases 1 (base case), 2 (base case) and 3 (gas reinjection). The curve of the base of study case 1 is similar to the curve derived from the decline curve rate-time equations of Arps for b = 0.

Table 5
Values of maximum potential and initial volume in place used to compute the curve of current dimensionless potential recovery factor for the Ormen Lange field.

$q_{pp,max}$ [1E09 Sm^3 /month]	2.52
G [1E09 Sm^3]	495.96

6. Field production of associated products (gas, water, condensate)

The curve of current dimensionless potential versus recovery factor is made based on the preferred phase of the reservoir, either oil or gas. The rates of associated products can be computed with the rate of the preferred phase and the producing gas-oil ratio (R_p), the condensate gas ratio or the producing water cut (W_c). The rate of the preferred phase will be the production potential (if the field is in decline) or any value below it.

The gas-oil ratio and water cut of the field can often be expressed as a function of recovery factor only. As an example, Fig. 9 presents the behavior of producing gas-oil ratio and water cut obtained in study case 2: base case, natural depletion and gas injection with VRR = 100%.

Several scenarios of gas or water coning and breakthrough could be captured by modifying base-case curves of water cut and gas-oil ratio versus recovery factor.

7. Discussion

In section 2, values of current dimensionless potential were extracted from models in study cases 1, 2 and 3. Study cases 1 and 2 use a tank model to represent the reservoir, while study case 3 employs a reservoir simulator. The flow in wellbores, flowlines, and pipelines is captured using steady-state models. Fluids considered are dry gas, saturated and undersaturated oil with associated production of gas and water. All cases employ pseudo-steady state inflow performance relationships.

The curve of current dimensionless potential versus recovery factor remained unchanged when initial surface volumes in place were varied. Changes to the production system downstream the near-wellbore region,

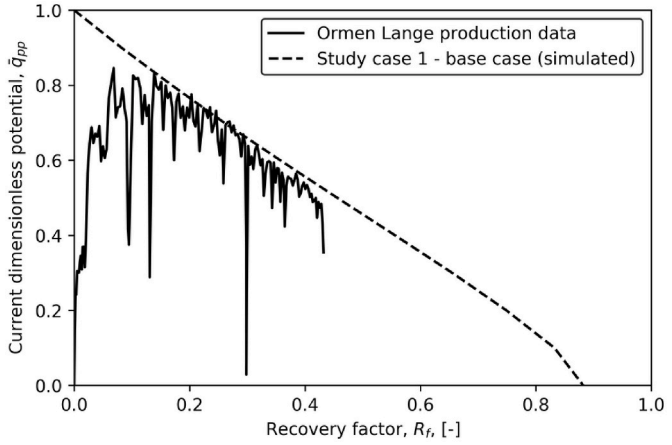

Fig. 8. Curves of current dimensionless potential rate ($\bar{q}_{pp}$) vs. recovery factor (R_f), derived from production data of the Ormen Lange field published by the Norwegian Petroleum Directorate and base case curve of study case 1. The curves are similar.

e.g. number of wells, surface gathering network, wellbore, well artificial lift, well productivity index cause modest variations to the curve of current dimensionless potential versus recovery factor. Changes to the reservoir recovery strategy and pressure support, and on the elements considered in the flow path between reservoir to separator significantly impact the curve of current dimensionless potential versus recovery factor. The recovery factor where the current dimensionless potential becomes zero depends on the pressures of the upstream and downstream boundary nodes of the model (i.e. reservoir and separator pressures).

The negligible impact of varying the initial surface volumes in place on the curve could be because the production potential depends mainly on reservoir pressure and reservoir pressure depends on the recovery factor. For example, whether the reservoir is large or small, it will reach the same reservoir pressure at the same recovery factor. However, for the large reservoir, this entails producing significantly more volumes than for the small reservoir.

This observation could be of great advantage during early field development phases where there are large uncertainties in the initial volumes in place. Still, the initial reservoir pressure is known with reasonable accuracy. The curve of current dimensionless potential versus recovery factor can be considered invariant, but probabilistic analyses can be performed by simply changing the value of initial surface volume in place (e.g. using probabilistic sampling).

The modest impact of changes to the production system downstream the near-wellbore region on the curve of current dimensionless potential could be due to the normalization by the upper bound of the production potential. For example, adding one more well will increase the production potential of the system at all recovery factors, but then the initial production potential is also increased. The numerator and denominator are therefore increased in more or less the same proportion. However, it is still remarkable that the effect of these changes on the curve are modest. For example, deploying gas lift on all wells does increase the field rates significantly (and on many occasions, it is needed to achieve economic production). Still, the normalized curve exhibits a very modest improvement when compared against the case with natural

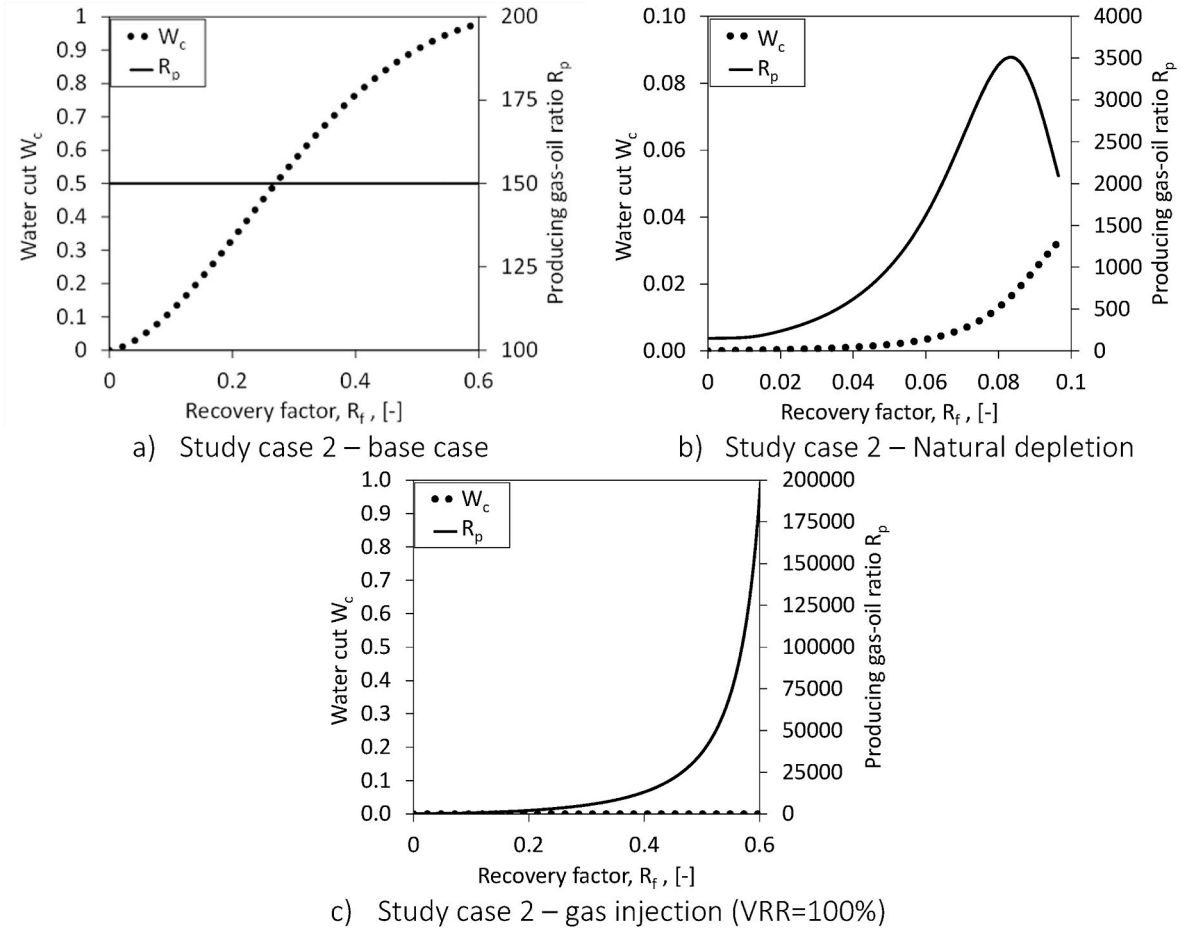

Fig. 9. Curves of producing gas-oil ratio (R_p) and water cut (W_c) vs. recovery factor (R_f) derived from the results of study case 2: a) water injection, (voidage replacement ratio VRR = 100%), b) Natural depletion, c) Gas injection (VRR = 100%).

flowing wells.

This observation could be exploited in cases where there are uncertainties in the production performance of the system, e.g., productivity of wells, the uptime of wells, and other components. The curve of current dimensionless potential versus recovery factor can be considered unique, but probabilistic analyses can be performed by simply changing the value of the maximum production potential (e.g. using probabilistic sampling).

However, the elements considered in the flow path from reservoir to separator seem to have a big impact on the curve. This could be because the wellbore, flowline and pipeline equations, when coupled with the reservoir model, change the physical behavior of the system fundamentally. This is a significant finding that confirms the importance of considering the production system downstream the sand face when predicting field performance and using a proper separator pressure.

The actual complexity and parameters of the wellbore-flowline system (e.g. the parallel paths from reservoir to separator, the system characteristics, like tubing size) seem to have a reduced impact on the curve of dimensionless potential.

Separator pressure affects the end point of the curve of current dimensionless potential. When there is no flow, there is only a hydrostatic column of fluid between reservoir and production. A higher separator pressure means that the reservoir pressure for no production must also be higher; thus the recovery factor achieved is lower.

Initial reservoir pressure affects the end point of the curve for the same reason mentioned above. If initial reservoir pressure is higher, then the recovery factor must be higher to achieve the pressure for which it is in hydrostatic equilibrium with the separator.

In some cases, reservoir pressure could also affect the rest of the curve. For example, for an undersaturated oil reservoir producing by natural depletion, the curves should be different if initial pressure is 20 or 200 bara above saturation pressure. However, this was not studied in the current work.

The curves of current dimensionless potential of study cases 3.1 and case 2.11 with VRR of 84% were significantly different. Both cases are undersaturated oil reservoirs undergoing gas injection and using coupled models of reservoir and network. This work did not study the reason for this difference if due to model input or due to the reservoir modeling approach. However, it indicates that it might not be appropriate to assume universal current dimensionless potential curves for certain types of reservoir and recovery strategies.

In section 3, two applications of the curves of current dimensionless field potential versus recovery factor were presented: computation of production profiles and estimation of plateau duration. The method described to compute production profiles reproduces with acceptable accuracy the model output of study case 3 when varying plateau rate and initial oil in place. This corroborates the observations made earlier by Gonzalez et al. (2019) and Angga (2019).

This is an interesting fact that hints that one could avoid running the detailed model several times in sensitivity, probabilistic or optimization analyses and use the curve of current dimensionless potential instead. However, the reservoir model employed is somewhat simple, i.e. is box-shaped, has high and uniform permeability (400 md) and porosity, has a small number of grid blocks. Therefore, extrapolation of these observations to other cases should be studied carefully. However, Gonzalez (2020) used a reservoir model with geological heterogeneity and the prediction of future performance using production potential curves still had an acceptable accuracy.

However, one can envision cases where using production potential proxies could not be appropriate to forecast future performance. For example, production potential curves are computed by producing the system always at its maximum. Therefore, at a given recovery factor, each well has a specific cumulative production. However, in the actual case, unless always produced at potential, the well cumulative production at a given recovery factor might not necessarily be the same as that of the production potential curve. This could potentially cause the production potential to be different between the actual system and the value reported in the curve. For example, if in actual production a particular well produced more than others causing early water breakthrough, then the production potential of the system will probably be smaller than that of the curve. This is due to the presence of water in the downstream gathering system. When using a material balance to represent the reservoir, this is not an issue because all wells usually produce the same gas-oil ratio and water cut.

The use of current dimensionless production potential curves could handle situations where there is well scheduling or where there are changes to the production system. In case changes do not affect the current dimensionless potential curve, one is only required to update the value of the maximum production potential corresponding to the change. A method to do this when there is well scheduling is outlined in section 3. However, when changes affect the shape of the current dimensionless potential curve, both curve and the value of the maximum production potential must be updated.

The method described in the previous paragraph will most likely not be valid to account for changes to the recovery mechanism (e.g. natural depletion, gas, or water injection). For example, it might not be appropriate to model a case with natural depletion and subsequent water injection by switching between two curves, one considering solely natural depletion and one solely water injection. This is because the starting point of the water injection process (reservoir pressure, oil, gas, and water saturation) is different in both cases.

In section 4, the integration and manipulation of Arps decline equations to compute expressions of current dimensionless potential give equations similar in structure to the equations fit to the results of study cases 1 and 3. However, a graphical comparison of these expressions against the results of study cases 1, 2, and 3 shows that for most cases (except case 1) is not possible to achieve a representative match by changing the decline constant (b) only. Moreover, expressions with $b > 0.25$ (Fig. 7a and 7.b) and $b > 0.5$ (Fig. 7c and 7 d) gave a maximum recovery factor ($R_{f,max}$) greater than one, which is physically nonsensical.

Several of the current dimensionless potential curves computed in study cases 1, 2, and 3 exhibits a change in concavity with the recovery factor. Curve concavity can be expressed using the second derivative of the current dimensionless potential with respect to recovery factor $\frac{d^2\overline{q}_{pp}}{dR_f^2}$. This term has been derived for all expressions presented in Table 4 and is presented in Eq. (8).\

$$\frac{d^2\overline{q}_{pp}}{dR_f^2} = \left\{ \begin{array}{c} Exponential \rightarrow 0 \\ Hyperbolic \rightarrow F^2 \cdot b \cdot \left(1 - F \cdot (1-b) \cdot R_f\right)^{\frac{2b-1}{1-b}} \\ Harmonic \rightarrow F^2 \cdot e^{-R_f \cdot F} \end{array} \right\} \quad (8)$$

The exponential decline expression is inadequate to fit curves of current dimensionless potential that exhibit significant concavity. The harmonic decline expression could be adequate to fit convex curves only ($\frac{d^2\overline{q}_{pp}}{dR_f^2} \geq 0$). From numerical tests run by the author, by varying b and R_f in the range 0–1 and F from −10 to 10, it seems the hyperbolic decline expression could be adequate to fit convex curves only.

Decline curve models for boundary dominated flow could be quality controlled and fine-tuned by comparing them against the curve of current dimensionless potential of the system.

In Section 5, the production data of Ormen Lange seems to exhibit roughly a linear trend between current dimensionless field potential and recovery factor after making reasonable assumptions and back-calculations of initial gas in place and initial production potential. This is somewhat expected because Ormen Lange is a single unit, dry gas reservoir.

However, this case demonstrates some of the challenges one might encounter when trying to derive the curve from field data or to tune field data to an equation. During the life of a real field there will unavoidably

be changes to the production system, e.g. well shut-in, well choking, drilling new wells, etc. To generate the curve of current production potential versus recovery factor, each field production record must be divided by the production potential of that system at initial time. In the example presented, all production records were divided by a unique value, thus yielding fluctuations in the curve, e.g. due to temporary shut-in of wells. Therefore, in such cases, it is not appropriate to apply a trendline to all production records to compute the current dimensionless potential.

It is important to highlight that the production records considered should be taken when the field is producing at production potential, at not during the constant rate period.

Section 6 shows that if the field's producing oil and gas ratios can be expressed as a function of recovery factor only, the current dimensionless potential of the associated phases can be computed using the ratio and the curve of dimensionless potential of the main phase.

However, the producing gas oil-ratio of the field at a given recovery factor will often depend on how much is produced from each well to achieve that recovery factor. For example, in a saturated oil field with gas cap with several wells where they are completed at different distances to the gas oil contact.

8. Remarks

The curve of current dimensionless potential versus recovery factor will probably not remain unique and the method proposed to compute production profiles will not work properly for cases where:

- The reservoir has low permeability, and a large part of the production occurs in the infinite-acting transient regime. For example, the curve derived by running an open-choke simulation at all times will most likely not capture the actual production potential correctly at a given recovery factor. If at a given recovery factor, the well was suddenly put to production after being shut-in, the instantaneous rate achieved could be significantly higher than the value provided by the curve.
- Systems with wells producing from multiple non-communicating reservoir units tied into a common gathering network (as discussed by Angga, 2019).

Points of interest for future work are:

- Compute curves of current dimensionless potential for other models and systems and evaluate their applicability to predict future performance
- Evaluate the effect of relative permeability curves and fluid properties on the curves of current dimensionless potential
- Study cases where the reservoir drive mechanism is changed during the lifetime of the field (e.g. when the field is initially produced with natural depletion and later produced using water injection)

9. Conclusions

Some coupled models or reservoir, well and network of hydrocarbon production systems exhibit a unique curve of current dimensionless potential versus recovery factor. In the cases tested the reservoir is represented with a tank model or is fairly homogeneous and structurally and spatially "simple" and all wells are producing from the same reservoir unit.

For the model types mentioned above, the curve of current dimensionless potential versus recovery factor of some hydrocarbon production systems exhibits a modest, or no variation at all when parameters about wells and gathering network, and initial surface volumes in place are modified. However, the curve is highly dependent on the pressure support strategy of the reservoir, i.e. the injection strategy and injection fluids and on the model elements considered in the flow-path from reservoir to processing facilities. The curves are also dependent on the pressure at the upstream and downstream boundaries of the model.

The procedure proposed to estimate production profiles from curves of current dimensionless potential versus recovery factor satisfactorily represents, for practical purposes, the output of simulations performed with the original model from which the curve was generated.

Procedures using dimensionless potential curves are suggested to generate production profiles when there are changes to the production system over the lifetime of the field and to allocate production between reservoir units to maximize field plateau duration.

The curves of current dimensionless production versus recovery factor could be used in a variety of engineering workflows, hopefully saving time, avoiding unnecessary sensitivity runs, and without significant compromises in accuracy.

The expressions of current dimensionless potential versus recovery factor derived from the decline curve rate-time equations of Arps, are similar in structure to some of the equations fit data from the study cases. However, it was not possible to reproduce the curves derived from the study cases (except for the dry gas case) by changing the b factor only.

Author contribution

I, Milan Stanko, I am the sole author of this work. I was in charge of Conceptualization; Data curation; Formal analysis; Investigation; Methodology; Project administration; Resources; Software; Supervision; Validation; Visualization; Roles/Writing - original draft; Writing - review & editing.

Declaration of competing interest

The authors declare that they have no known competing financial interests or personal relationships that could have appeared to influence the work reported in this paper.

Data availability

Model and results of study cases 1,2 and 3, and other models and results shown in this article are available online in the following address: https://drive.google.com/open?id=12j8mPNjboEzVgipd6iVSKdxYdraXZsyv.

An executable program (compatible with Windows operating systems only) is provided here: https://drive.google.com/open?id=156uPsXD_k5EJKkxYCN8StJEb5ZjZODkQ to compute production profiles of oil, gas and water using the following input:

- fluid type (oil or gas)
- initial volume in place
- maximum production potential
- table of desired production schedule (time-rate)
- table of modifications to the production system in time (time – fraction). The fraction represents the increase or decrease in the maximum production potential due to changes in the system
- table of R_p and W_c versus recovery factor (if oil)
- table of dimensionless production potential versus recovery factor

Instructions of use: Download all files to your computer and extract to a common directory. Double-click on the exe file to run the program and follow the instructions. Use at your own judgement. This tool was not used in this article.

Declaration of Competing Interest

The authors declare that they have no known competing financial interests or personal relationships that could have appeared to influence the work reported in this paper.

Acknowledgements

The author would like to thank former master student I Gusti Agung Gede Angga for creating the models of study case 2 and to the company AkerSolutions for providing data to I Gusti Agung Gede Angga to build the models.

Nomenclature

3D	three-dimensional
b	decline constant for Arps rate-time decline equations
B_o	oil volume factor, [m^3/Sm^3]
B_g	gas volume factor, [m^3/Sm^3]
C_{fl}	flowline coefficient [Sm^3/d/bara]
C_o	oil compressibility [1/psi]
C_{tub}	tubing coefficient [Sm^3/d/bara]
d	days
d_{fl}	flowline diameter [m]
d_{tub}	tubing diameter [m]
D_i	initial decline rate, [1/d]
F	factor to define D_i as a function of initial volume in place Q
g	gravitational acceleration 9.81 [m/s^2]
G	initial gas in place, [Sm^3]
G_p	cumulative gas production [Sm^3]
GL	Gas lift
GI	gas injection
h	reservoir layer height [m]
ID	inner diameter [m]
IPR	inflow performance relationship
k	absolute permeability [D]
k_{rg}	relative permeability of gas
k_{ro}	relative permeability of oil
k_{rw}	relative permeability of water
L	conduit length [m]
M_{air}	molecular weight of air [28.97 kg/kmol]
MD	Measured depth [m]
n	inflow backpressure exponent [-]
N	initial oil in place, [Sm^3]
N_p	cumulative oil production [Sm^3]
net	network
p	pressure, [bara]
p_{sc}	standard condition pressure (1.01325 $bara$)
p_{wf}	bottom-hole flowing pressure [bara]
p_{wh}	wellhead flowing pressure [bara]
$\overline{q}_{pp}$	current dimensionless potential of oil or gas [-]
$q_{pp,max}$	upper bound of the current dimensionless potential [-]
q_i	maximum flow rate of oil or gas at initial pressure [Sm^3/d]
$q_{plateau}$	plateau rate or oil or gas [Sm^3/d or stb/d]
Q	initial oil (or gas) in place, [Sm^3]
Q_p	cumulative oil (or gas) production [Sm^3]
r	radius [m]
R	universal gas constant, 8314.46 J/kmol K
R_f	recovery factor [-]
R_p	gas oil ratio [Sm^3/Sm^3]
R_s	solution gas-oil ratio [Sm^3/Sm^3]
s	skin [-]
S	tubing elevation coefficient [-]
S_g	gas specific gravity [-]
t	time, [d]
$t_{plateau}$	plateau duration [d]
T	temperature [K]
T_{sc}	standard condition temperature (15.56 C)
T_R	reservoir temperature [C]
T_{wh}	wellhead flowing temperature [C]
T_{sep}	separator temperature [C]
TVD	True vertical depth [m]
VRR	Voidage replacement ratio [-]

W_c	water cut [-]
Z	gas deviation factor [-]

Symbols

α	inclination angle of conduit with respect to horizontal [rad]
ΔX	cell size in X direction [ft]
ΔY	cell size in Y direction [ft]
ΔZ	cell size in Z direction [ft]
π	constant, (3.1416)
μ	fluid viscosity [cP]

Subscripts

av	average
e	external boundary
fl	flowline
i	initial
plateau	plateau
R	reservoir
ref	reference conditions, standard conditions
sep	separator
tub	tubing
w	well

Superscripts

j	generic time step "j"
i	initial

Units conversion

1 bar	14.5038 psi
1 BTU	1055.06 J
(1 °C X 9/5) + 32	°F
1 cP	0.001 Pa s
1 in	0.0254 m
1 m	3.2808 ft
1 m^3	6.2898 bbl
1 m^3	35.3147 ft^3

Appendix A. Data from study case 1, Dry gas system

Consider a production system where there are "x" identical wells producing from a common dry gas reservoir, each one with their own separator and horizontal flowline. The dry gas tank material balance equation is:

$$p_R = \frac{Z_R \cdot p_i}{Z_i} \cdot \left(1 - \frac{G_p}{G}\right) \quad \text{1-1}$$

The well inflow performance relationship:

$$q_w = \frac{7.84 \cdot k \cdot h \cdot \left(m(p_R) - m\left(p_{wf}\right)\right)^n}{T_R \cdot \left(ln\left(\frac{r_e}{r_w}\right) - 0.75 + s\right)} \quad \text{1-2}$$

m is the pseudo-pressure function

$$m(p) = \int_{p_{ref}}^{p} \frac{p}{Z \cdot \mu} dp \quad \text{1-3}$$

The dry gas tubing equation is:

$$q_w = C_{tub} \cdot \left(\frac{{p_{wf}}^2}{e^S} - {p_{wh}}^2\right)^{0.5} \quad \text{1-4}$$

with C_{tub}:

$$C_{tub} = \left(\frac{\pi}{4}\right) \cdot \left(\frac{R}{M_{air}}\right)^{0.5} \cdot \left(\frac{T_{sc}}{p_{sc}}\right) \cdot \left(\frac{{d_{tub}}^5}{f_M \cdot L_{tub} \cdot S_g \cdot Z_{av} \cdot T_{av}}\right)^{0.5} \cdot \left(\frac{S \cdot e^S}{e^S - 1}\right)^{0.5} \quad \text{1-5}$$

And the tubing elevation factor S:

$$S = 2 \cdot \frac{M_g}{Z_{av} \cdot R \cdot T_{av}} \cdot L_{tub} \cdot g \cdot \cos(\alpha)$$

The flowline (or pipeline) equation (assuming horizontal configuration):

$$q_w = C_{fl} \cdot \left({p_{wh}}^2 - {p_{sep}}^2 \right)^{0.5} \quad \text{1-6}$$

where

$$C_{fl} = \left(\frac{\pi}{4}\right) \cdot \left(\frac{R}{M_{air}}\right)^{0.5} \cdot \left(\frac{T_{sc}}{p_{sc}}\right) \cdot \left(\frac{{d_{fl}}^5}{f_M \cdot L_{fl} \cdot S_g \cdot Z_{av} \cdot T_{av}}\right)^{0.5} \quad \text{1-7}$$

The Moody friction factor (f_M) is taken from the correlation of R. V. Smith (1950) for gas wells. $f_M = \frac{0.0077}{d^{0.224}}$
The gas deviation factor Z has been calculated with the correlation of Hall and Yarborough (1973).
The gas viscosity has been calculated with the correlation of Lee et al. (1966).
Base case input:

- Number of wells $= 5$
- Initial gas in place $G = 2.7 \cdot 10^{11}\ Sm^3$
- Initial reservoir pressure, $p_i = 276\ bara$
- Reservoir temperature $T_R = 90\ ^\circ C$
- Gas specific gravity $S_g = 0.5$
- Inflow backpressure exponent, $n = 1$
- Product permeability -layer height k h = 2030 [md m]
- Well skin, s = 3 [-]
- Wellbore radius, $r_w = 0.11$ [m]
- External radius, $r_e = 453.85$ [m]
- Well inclination from the horizontal $= \pi \cdot 0.5$ [rad]
- Tubing inner diameter, $d_{tub} = 0.15$ [m]
- Tubing length, $L_{tub} = 3000$ [m]
- Wellhead temperature $T_{wh} = 70$ [°C]
- Flowline inner diameter, $d_{fl} = 0.1524$ [m]
- Flowline length, $L_{fl} = 10\,000$ [m]
- Separator temperature $T_{sep} = 60$ [°C]
- Separator pressure, $p_{sep} = 30\ bara$

Network case input:

- Wellhead temperature $T_{wh} = 70$ [°C]
- Flowline inner diameter, $d_{fl} = 0.154$ [m]
- Flowline length, $L_{fl} = 5\,000$ [m]
- Pipeline inner diameter, $d_{pl} = 0.508$ [m]
- Pipeline length, $L_{pl} = 60\,000$ [m]
- Separator temperature $T_{sep} = 30$ [°C]
- Separator pressure, $p_{sep} = 30\ bara$

Table 1.1
Values of flowing bottom-hole pressure imposed on the model with IPR only to reproduce the values of the curve of current dimensionless potential versus recovery factor of the base case

R_F	p_{wf}
[-]	[bara]
0.000	241
0.078	218
0.161	195
0.248	171
0.339	148
0.432	124
0.528	101
0.625	78
0.721	56
0.874	35

Appendix B. Data from study case 2

Table 2.1
Well characteristics.

Water depth [m]	120
Well MD/TVD [m]	3500/2500
Well drainage radius [m]	800
Wellbore radius [m]	0.12
Skin factor [-]	+5
Tubing ID [m]	0.124
Tubing roughness [m]	1.5 E−5
Gas lift valve depth [m]	3000
Max gas lift injection rate per well [1000 Sm^3/d]	400
Formation temperature at seabed [°C]	5
Productivity index, J, well 1,4,7 and base case [$Sm^3/d/bar$]	67.36
Productivity index, J, well 2 and 5 [$Sm^3/d/bar$]	101.04
Productivity index, J, well 3 and 6 [$Sm^3/d/bar$]	33.68

Table 2.2
Reservoir parameters.

Permeability [mD]	250
Porosity [-]	0.18
Reservoir thickness [m]	50
Initial water saturation	0.25
Irreducible water saturation [-]	0.25
Residual oil saturation [-]	0.25
Residual gas saturation [-]	0
End point k_{rw}	0.8
End point k_{ro}	0.8
End point k_{rg}	0.8
Corey exponent for water [-]	1.5
Corey exponent for oil [-]	1.5
Corey exponent for gas [-]	1.5
Initial reservoir pressure [bara]	280
Reservoir temperature [°C]	80
N [M Sm^3]	55
Aquifer volume [M m^3]	20
Rock compressibility [bar^{-1}]	5.32E-5

Table 2.3
Fluid properties.

Variable	value
Solution gas-oil ratio [Sm^3/Sm^3]	150
Oil density [kg/m^3]	850
Gas specific gravity	0.75
Saturation pressure at reservoir conditions [bara]	257.3
Gas lift gas specific gravity [-]	0.7

Table 2.4
Fluid properties – black oil correlations.

Variable	Correlation
P_b, R_s, B_o	Glasø
μ_o	Beal et al.
C_o	Vasquez and Beggs
B_g	Z obtained from Standing Katz

Table 2.5
Subsea network characteristics.

Ambient temperature [°C]	5
Overall pipe heat transfer coefficient [W/m^2 K]	4
Length of horizontal pipeline to facilities [m]	30 000
ID of horizontal pipeline to facilities [m]	0.45
Length of riser from seabed to facilities [m]	400
ID of riser from seabed to facilities [m]	0.45
Length of flowline from template 1 to pipeline [m]	5000
ID of flowline from template 1 to pipeline [m]	0.45
Length of flowline from template 2 to pipeline [m]	5000
ID of flowline from template 2 to pipeline [m]	0.45

Appendix C. Data from case 3

Table 3.1
Well characteristics.

Well MD/TVD [ft]	11 000
Wellbore radius [ft]	0.345
Skin factor [-]	0
Tubing ID [in]	4.99
MD of tubing bottom [ft]	10 900
Casing ID [in]	6.184
MD of casing bottom [ft]	11 000
Tubing roughness [in]	6E-4
Formation temperature at seabed [°F]	50
Producer 1 cell indexes	6,8,1-10
Producer 2 cell indexes	14,8,1-10
Producer 3 cell indexes	6,14,6-10
Producer 4 cell indexes	14,14,6-10
Injector 1 cell indexes	10,11,1-10
Injector 2 cell indexes	19,11,1-10
Injector 3 cell indexes	10,5,1-10
Injector 4 cell indexes	10,17,1-10

Table 3.2
Reservoir parameters.

Permeability (uniform) [mD]	400
Porosity [-]	0.25
Reservoir thickness [ft]	200
Relative permeability model	Stone I
Critical water saturation (Swc)	0.2
Critical oil-water saturation (Sowc)	0.2
Critical oil-gas saturation (Sogc)	0.02
Critical gas saturation	0.01
End point k_{rw}, exponent	0.6,1.8
End point k_{row}, exponent	0.8,0.7
End point k_{rog}, exponent	0.8,0.7
End point k_{rg}, exponent	0.1,1
Initial reservoir pressure [psig]	9800
Oil-water capillary pressure [psi]	0
Gas-oil capillary pressure [psi]	0
Reference depth [ft]	11 000
Reservoir temperature [°F]	200
N [stb]	6.83 E+08
Rock compressibility [psi^{-1}]	1E-5
Number of cells in x	21
Number of cells in y	20
Number of cells in z	10
ΔX [ft]	548
ΔY [ft]	570
ΔZ [ft]	20

Table 3.3
Fluid properties.

Variable	value
Solution gas-oil ratio [scf/stb]	650
Oil API gravity	39
Gas specific gravity	0.67
Water specific gravity	1.03
Saturation pressure at reservoir conditions [psia]	3304.7

Table 3.4
Fluid properties – black oil correlations.

Variable	Correlation
P_b, R_s, B_o	Vasquez and Beggs
μ_o	Beggs et al.
C_o	Vasquez and Beggs
B_g	Z obtained from Standing Katz

Table 3.5
Surface gathering network characteristics.

Ambient temperature [°F]	50
Overall pipe heat transfer coefficient [BTU/h/ft^2/F]	8
Length of horizontal pipeline to facilities [ft]	3500
ID of horizontal pipeline to facilities [in]	16
Length of flowline from template 1 (producers 1 and 2) to pipeline [ft]	0
Length of flowline from template 2 (producers 3 and 4) to pipeline [ft]	1000
ID of flowline from template 2 (producers 3 and 4) to pipeline [m]	12

References

Al-Shaalan, T.M., Dogru, A., Fung, L., 2002. Coupling the reservoir simulator Powers with the surface facilities' network simulator Pipesoft. Saudi Aramco J Technol Fall 13–21, 2002.

Ali, S.M.F., Nielsen, R.F., 1970. The material balance approach vs reservoir simulation as an aid to understanding reservoir mechanics. In: SPE-3080, Presented at the Fall Meeting of the Society of Petroleum Engineers of AIME, 4–7 October. Society of Petroleum Engineers, Houston, Texas, USA. https://doi.org/10.2118/3080-MS.

Angga, I.A.G., 2019. Automated Decision Support Methodology for Field Development: the Safari Field Case. Norwegian University of Science and Technology (NTNU). Master Thesis. Trondheim, Norway.

Arps, J.J., 1945. Analysis of decline curves. Trans., AIME 160, 228–247.

Barroux, C.C., Duchet-Suchaux, P., Samier, P., de France, R.N.G., 2000. Linking reservoir and surface simulators: how to improve the coupled solutions. In: SPE-65159-MS, Presented at the SPE European Petroleum Conference, 24–25 October. France, Society of Petroleum Engineers, Paris. https://doi.org/10.2118/65159-MS.

Fetkovich, M.J., 1980. Decline Curve Analysis Using Type Curves. Society of Petroleum Engineers. https://doi.org/10.2118/4629-PA.

Gonzalez, D., 2020. Methodologies to Determine Cost-Effective Development Strategies for Offshore Fields during Early-phase Studies Using Proxy Models and Optimization. Norwegian University of Science and Technology (NTNU), Trondheim, Norway. PhD dissertation.

González, D., Stanko, M., Hoffmann, A., 2019. Decision support method for early-phase design of offshore hydrocarbon fields using model-based optimization. J Petrol Explor Prod Technol. https://doi.org/10.1007/s13202-019-0613-1.

Haldorsen, H.H., 1996. Choosing between rocks, hard places and a lot more: the economic interface. In: Dore, A.G., Sinding-Larsen, R. (Eds.), Quantification and Prediction of Hydrocarbon Resources.

Hall, K.R., Yarborough, L., 1973. A new EOS for Z-factor calculations. Oil Gas J. 18. June. 82.

Holanda, R.W.D., Gildin, E., Jensen, J.L., Lake, L.W., Kabir, C.S., 2018. A state-of-the-art literature review on capacitance resistance models for reservoir characterization and performance forecasting. Energies 11 (12), 3368.

Jahn, F., Cook, M., Graham, M., 2008. Hydrocarbon Exploration and Production, Developments in Petroleum Science. Elsevier, Amsterdam.

Lee, A.L., Gonzalez, M., Eakin, B.E., 1966. The Viscosity of Natural Gases. Journal of Petroleum Technology. Norwegian Petroleum Society Special Publications, vol. 6. Elsevier, Amsterdam, pp. 291–312. https://doi.org/10.1016/S0928-8937(07)80025-7.

Norwegian Petroleum Directorate, 2020. Facta pages. Retrieved from. https://factpages.npd.no/nb-no/field/tableview/production/saleable/monthly.

Petroleum Experts, 2019. Integrated Petroleum Management Software IPM - Release Notes v12.0.

Smith, R.V., 1950. Determining friction factors for measuring productivity of gas wells. Trans AIME 189 (73).

Undeland, E., 2012. Residual Gas Mobility in Ormen Lange. Norwegian University of Science and Technology (NTNU). Master Thesis. Trondheim, Norway.

Valbuena, E., Barrufet, M., Killoug, J., 2015. Forecasting production performance in reservoir-network coupled systems with asphaltene modeling. SPE-174795. In: Presented at the SPE Annual Technical Conference and Exhibition Held in Houston, Texas, USA, 28–30 September. Society of Petroleum Engineers. https://doi.org/10.2118/174795-MS.

Yin, Z., MacBeth, C., Chassagne, R., Vazquez, O., 2016. Evaluation of inter-well connectivity using well fluctuations and 4D seismic data. J. Petrol. Sci. Eng. 145, 533–547.